Medicinal chemistry

Sampaio et al, Med chem 2014, 4:11
DOI: 10.4172/2161-0444.1000226

Research Article Open Access

Synthesis, Antiproliferative and Anti-inflammatory Activities of Novel Simplified Imatinib Analogues

Thiago Stevanatto Sampaio[1,2], Lídia Moreira Lima[1,2*], Renata da Silva Zardo[1,2], Cláudia Pessoa[3], Bruno Coêlho Cavalcanti[3], Rosane de Paula Castro[4], José Ricardo Sabino[4], Patrícia Dias Fernandes[1,2] and Eliezer J Barreiro[1,2*]

[1]*Instituto Nacional de Ciência e Tecnologia de Fármacos e Medicamentos, Laboratório de Avaliação e Síntese de Substâncias Bioativas, Universidade Federal do Rio de Janeiro, CCS, Cidade Universitária, Rio de Janeiro-RJ, Brazil*

[2]Programa de Pós-Graduação em Farmacologia e Química Medicinal, Instituto de Ciências Biomédicas, Universidade Federal do Rio de Janeiro, CCS, Cidade Universitária, Rio de Janeiro-RJ, Brazil

[3]Laboratório Nacional de Oncologia Experimental, Departamento de Fisiologia e Farmacologia, Faculdade de Medicina, Universidade Federal do Ceará, Fortaleza-CE, Brazil

[4]Instituto de Física, Universidade Federal de Goiás, Goiânia-GO, Brazil

Abstract

We described the synthesis of carboxamide derivatives designed as novel simplified imatinib analogues and their antiproliferative and anti-inflammatory activities. Compound 2c showed a unique conformation determined by X-ray diffraction and by NMR ^{1}H and displayed antiproliferative potency in the same magnitude order than the standard imatinib. Compounds 6-10 were prepared by structural modification in carboxamide 2c, and with exception of derivative 10, they were inactive as antiproliferative agent. However, these compounds showed same anti-inflammatory potency than imatinib, standing out carboxamide 9 that was six time more potent as TNF-α inhibitor production.

Keywords: Anti-inflammatory, Antiproliferative, Carboxamide, Imatinib analogues, TNF-α inhibitor

Introduction

Imatinib, the first tyrosine-kinase inhibitor to be approved for the treatment of cancer, mainly chronic myelogenous leukemia (CML) and gastrointestinal stromal tumors (GISTs) [1], is considered a milestone in small-molecule drug discovery and molecular targeted therapies. However, unlike the previous report, imatinib is not a specific inhibitor of ABL, but also inhibits PDGFRs, KIT, ARG (abl-related gene) and potentially other enzymes, which have not yet been tested [2].

Besides its antineoplastic effects, anti-inflammatory and anti-fibrotic activity has recently been assign to imatinib, revealing its multitarget profile [3-7]. However, its exact anti-inflammatory mechanism of action remains elusive. Nonetheless, its ability to down-regulate the expression of inflammatory cytokines, like TNF-α, IL-6 and IL-1β, has been considered a possible mechanism [4,6].

In this paper we describe the synthesis, antiproliferative and anti-inflammatory activities of novel carboxamide derivatives (2a-c) designed as simplified imatinib analogues (Figure 1) in order to obtain new anti-inflammatory drug candidates.

Results and Discussion

The carboxamide derivatives (2a-c) were planned by molecular simplification [8] in the structure of the prototype imatinib (1), resulting in the elimination of 4-(pyridin-3-yl)pyrimidin-2-amine moiety (Subunit A, Figure 1), followed by the classic ring isosterism and retroisosterism [9] of subunits B and C, respectively (Figure 1).

The regioisomers (2a-c) were synthesized in three linear steps depicted in Scheme 1. The synthetic route began with reductive amination step, involving the reaction of 2- or 3- or 4-nitrobenzaldehyde (3a-c) with 1-methylpiperazine in the presence of zinc chloride in methanol and sodium cyanoborohydride to obtain the nitrobenzyl-*N*-methyl-piperazines 4a-c in moderate yield [10]. Interconversion of functional group was carried out based on the reduction of nitro group in respective amine derivatives (5a-c), using metallic iron in the presence of slightly acid solution of ammonium chloride in water and ethanol (1:1) [11]. The condensation of the amines 5a-c with 2-quinaxaloyl chloride, at room temperature using dichloromethane

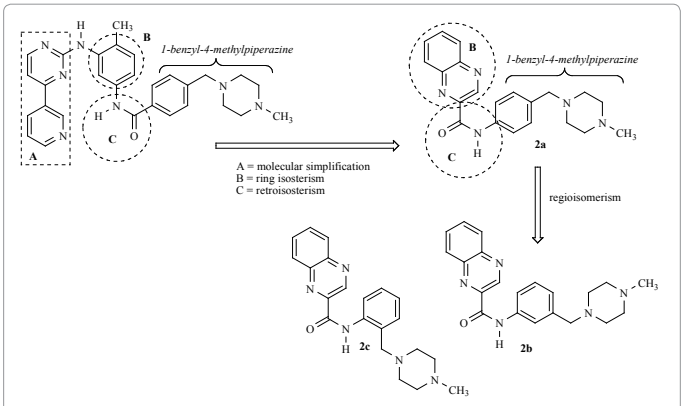

Figure 1: Design conception of carboxamide derivatives (2a-c) through molecular simplification from imatinib.

as solvent [12], obtained the desired carboxamides 2a-c in good yields (Scheme 1). The regioisomers 2a-c were fully characterized by ^{1}H NMR, ^{13}C NMR and IR spectroscopy and their purity was determined by elementar analysis or HPLC. The possible conformation differences, arising from the isomerism in the benzyl-*N*-methylpiperazine unit, were assigned based on the X-ray crystallographic studies performed with carboxamides 2a-c (Figure 2 and Table 1).

***Corresponding authors:** LM Lima, Laboratório de Avaliação e Síntese de Substâncias Bioativas, Universidade Federal do Rio de Janeiro, P.O. Box 68024, Zip code: 21944-971, Rio de Janeiro, RJ, Brazil, Tel.+55(21)39386503; E-mail: lidia@lassbio.icb.ufrj.br

EJ Barreiro, Laboratório de Avaliação e Síntese de Substâncias Bioativas, Universidade Federal do Rio de Janeiro, P.O. Box 68024, Zip code: 21944-971. Rio de Janeiro, RJ, Brazil, Tel.: +55(21)39386644; Fax: +55(21)39386478; E-mail: ejbarreiro@ccsdecania.ufrj.br

Received November 05, 2014; **Accepted** November 21, 2014; **Published** November 23, 2014

Citation: Sampaio TS, Lima LM, da Silva Zardo R, Pessoa C, Cavalcanti BC, et al. (2014) Synthesis, Antiproliferative and Anti-inflammatory Activities of Novel Simplified Imatinib Analogues. Med chem 4: 756-762. doi:10.4172/2161-0444.1000226

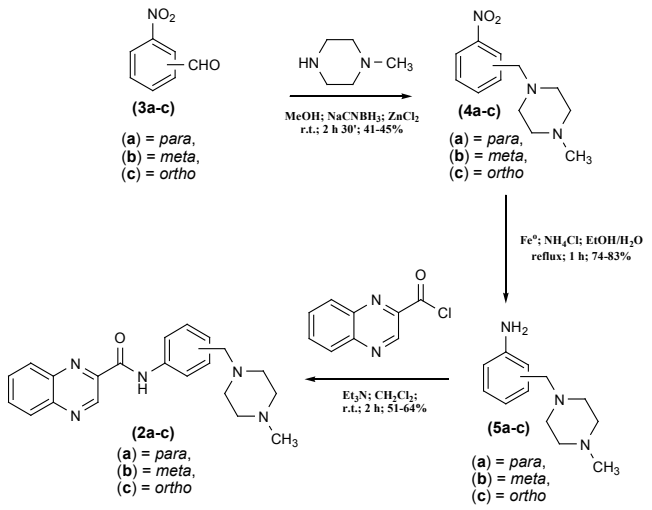

Scheme 1: Synthesis of compounds 2a-c.

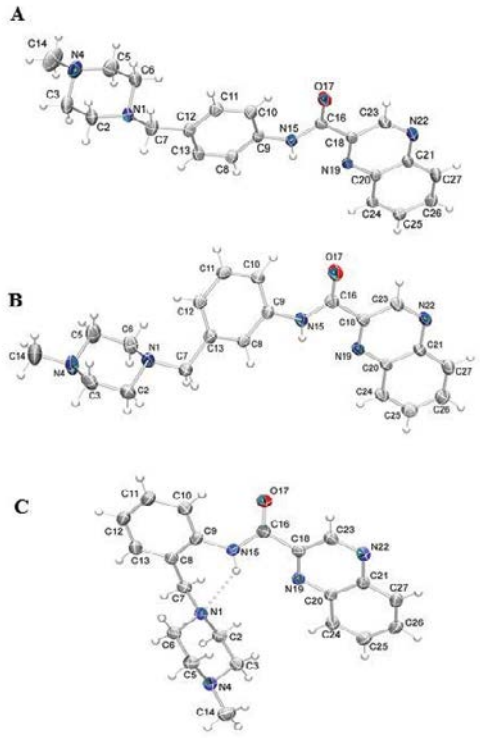

Figure 2: ORTEP view of compounds 2a-c with the atom displacement ellipsoids drawn at 30% of probability level. A) compound 2a; B) compound 2b; C) compound 2c.

Single crystals of compounds 2a-c were obtained and subjected to X-ray diffraction; the ORTEP [13] view is shown in Figure 2a-2c. The different positioning of the piperazine moiety leads to changes in the carboxamide fragment conformation in solid state. These changes occur in the angles between the planes passing through the atoms of the planar subunits quinoxaline C18/N19/C20/C24/C25/ C26/C27/ C21/N22/C23 (plane α), the acetamide bridge N15/C16/C18/O17 (plane β) and the phenyl ring C8/C9/C10/C11/C12/C13 (plane γ). The piperazine conformation relative to the phenyl ring is also subject to torsional strain about the σ-bonding between N1 atom and the methylene carbon C7, where the methylene´s hydrogen is eclipsed in 2a and 2c and staggered in 2b. Bond lengths are in good agreement between the three compounds. It is worth to notice that the density increases from compound 2a to 2c, showing that in compound 2c, the intramolecular N15-H15…N1 H-bond leads to a more compact molecular conformation when compared to 2a and 2b.

In order to establish the better regioisomer template to be elected as a new lead compound, with an original structural pattern, the antiproliferative activity of carboxamides 2a-c was investigated against HL-60 (human leukemia), SF-295 (human glioblastoma) and HCT-8 (human colorectal carcinoma) tumor cell lines [14]. In this assay, doxorubicin was used as positive control and imatinib as standard drug. As demonstrated in Table 2, the regioisomer *para* (2a) and *meta* (2b) were inactive, while the regioisomer *ortho* (2c) displayed antiproliferative potency similar to the prototype imatinib, against human colorectal carcinoma and human leukemia cells. In addition, compound 2c was not cytotoxic against healthy cells (*i.e.* human lymphocyte).

The differences in the antiproliferative activity of carboxamides 2a-c, especially the *ortho* regioisomer (2c), can be attributed to its unique conformation due to the presence of intramolecular hydrogen bond (N1 and H15) observed in the solid state, by X-ray diffraction (Figure 2C and Table 1), and confirmed in solution by ^{1}H NMR, through the differences in the chemical shift of the amide hydrogen (CONH) of compounds 2a-c. The NH proton signal for compounds 2a and 2b is seen at 9.75 and 9.79 ppm, while for compound 2c signal moves downfield to δ 11.7 ppm, due a deshielding effect promoted by the intramolecular

Compound	D—H...A	D—H	H...A	D...A	D—H...A
Intermolecular					
2a	C10—H10…O17^{iii}	0.93	2.33	3.259(2)	124
2b	N15—H15…N22^{iv}	0.93	2.33	3.259(2)	124
2c	C3—H3b...O17^{v}	0.97	2.52	3.270(2)	135
2c	C7—H7a...Cg1^{vii}	0.97	2.45	3.367(2)	157
Intramolecular					
2c	N15-H15...N1	0.86	2.24	2.915(2)	136
Symmetry operations: ^{iii}: 1-x,1-y,-z, ^{iv}: x, 3/2+y, ½+z, ^{v}: 1/2-x,1/2+y,1/2-z, ^{vii}: 1-x,1-y,-z Cg1: C18—N19—C20—C21—N22—C23					

Table 1: Hydrogen-bonds and intermolecular interactions geometry (Å,°).

Compound	Cell Lines – IC_{50} μM ± S.E.M			Primary culture
	HL-60	SF-295	HCT-8	Human Lymphocytes
2a (LASSBio-1599)	> 300	208.67 ± 7.28	173.41 ± 5.91	194.3 ± 2.17
2b (LASSBio-1598)	> 300	287.53 ± 3.15	> 300	> 300
2c (LASSBio-1597)	74.40 ± 9.80	107.64 ± 5.10	39.61 ± 7.05	> 300
6 (LASSBio-1724)	> 300	> 300	> 300	> 300
7 (LASSBio-1725)	> 300	> 300	> 300	> 300
8 (LASSBio-1726)	> 300	> 300	> 300	> 300
9 (LASSBio-1723)	> 300	> 300	> 300	> 300
10 (LASSBio-1727)	35.75 ± 2.51	> 300	> 300	> 300
Imatinib	22.81 ± 3.11	41.53 ± 5.73	34.03 ± 4.11	> 300
Doxorubicin	0.04 ± 0.01	0.48 ± 0.02	0.02 ± 0.01	0.37 ± 0.01

HL-60 (human leukemia); SF-295 (human glioblastoma); HCT-8 (human colorectal carcinoma)

Table 2: Antiproliferative activity of carboxamides 2a-c, imatinib and doxorubicin (positive control) against HL-60, SF-295, HCT-8 tumor cell lines and their cytotoxic activity against primary culture of human lymphocytes.

hydrogen bond between H15 (XONH) and N1 (piperazine), defining a six-membered ring (Figure 2C).

Once defined the *ortho* scaffold as the better template to achieve new imatinib analogues, the carboxamide 2c was modified varying the nature of the *N*-substituted piperazine (8-10) and by bioisosteric replacement [9] of the quinoxaline ring (6-7) (Figure 3). These analogues were synthesized applying the same methodology previously described for carboxamides 2a-c, exploring steps of reductive amination, functional group interconversion and condensation of amines with acyl chlorides derivatives (Scheme 2).

The analogues 6-10 were also evaluated as antiproliferative lead-candidates (Table 2). As show in Table 2 the attempt to replace the quinoxaline ring (2c) by the pyrazine system (6) or by the retroisoster 7 resulted in loss of activity. Also, the substitution of methyl group linked in the piperazine subunit by an aromatic group (phenyl or pyrimidine) resulted in failure of antiproliferative activity. However, compound 10, having a 1-(2-hydroxyethyl) piperazine unit, instead of the *N*-methylpiperazine presented in the lead 2c, seems to present a more selective cytotoxic profile, being active against human leukemia (HL-60) and inactive against the solid tumor cells lines SF-295 and HCT-8.

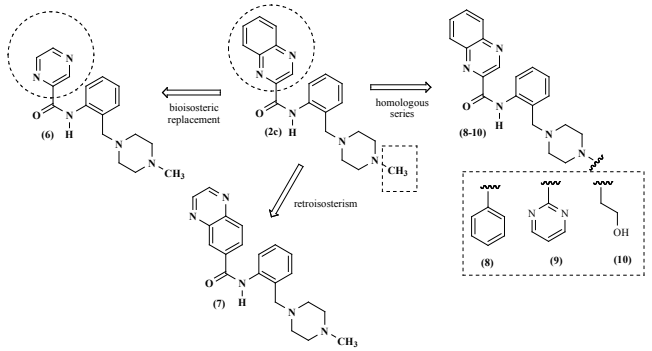

Figure 3: Design conception of carboxamide derivatives (6-10) from the prototype 2c.

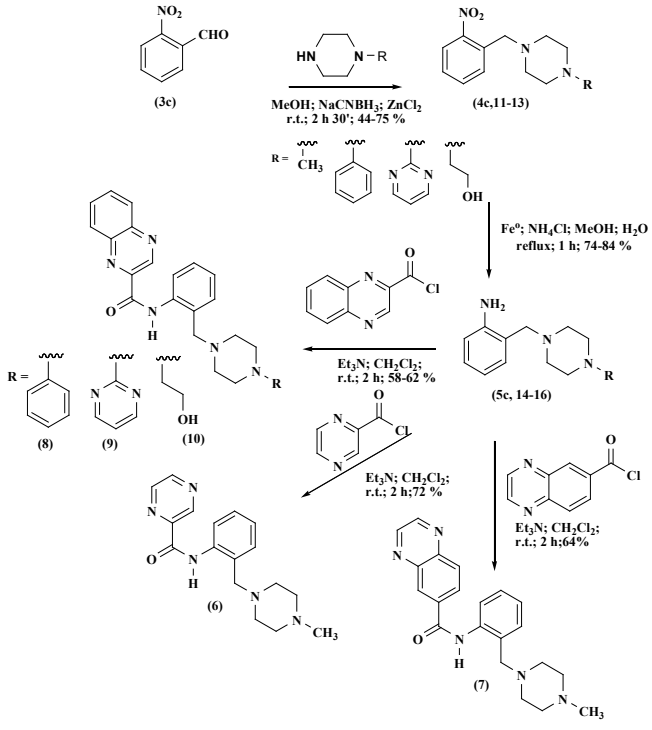

Scheme 2: Synthesis of compounds **6-10**

Considering the recent anti-inflammatory profile described for the prototype imatinib, the carboxamides 2c and 6-10 were studied in carrageenan-induced acute inflammation in the mouse air pouch synovial model [15]. In this model, the number of leukocytes recruited into the pouch increased progressively after carrageenan, and the ability of carboxamides derivatives and the prototype imatinib to inhibit the cell migration and to reduce the cytokine TNF-α production were investigated. As shown in Table 3, imatinib (1) and carboxamides 2c and 6-10, when administered *per os*, were able to inhibit the leukocyte migration revealing an important anti-inflammatory profile with ED_{50} (in μmol/kg) values similar to imatinib. In order to verify the anti-TNF-activity of these derivatives, we quantified the TNF-α produced in the SAP exsudate. As shown in Table 3, compound 9 standing out, showing ED_{50} value of 0.07 μmol/kg, being more potent than imatinib (ED_{50} value of 0.44 μmol/kg).

Conclusion

In summary, similar to imatinib (1) and the initial prototype 2c, all carboxamide derivatives described herein (6-10) showed an important anti-inflammatory and anti-TNF-α activity *in vivo*. Compound 9, having a pyrimidine group linked to piperazine ring was six times more potent as TNF-α production inhibitor than imatinib (1). It is noteworthy that modifications introduced in quinoxaline ring or piperazine unit were able to dissociate the anti-inflammatory effect in the detriment of the antiproliferative activity, as exemplified by compounds 6-9. From this series of simplified imatinib analogues, only compounds 2c and 10 showed both cytotoxic and anti-inflammatory activities.

Experimental Section

Chemistry

All commercially available reagents and solvents were used without further purification. Reactions were routinely monitored by thin-layer chromatography (TLC) in silica gel (F245 Merck plates) and the products visualized with ultraviolet lamp (254 and 365 nm). ^{1}H and ^{13}C nuclear magnetic resonance (NMR) spectra were determined in $CDCl_3$ solution using a Bruker AC-200. The chemical shifts are given in parts per million (δ) from solvent residual peaks and the coupling constant values (J) are given in Hz. Signal multiplicities are represented by: s, singlet; d, doublet; m, multiplet; Is, large signal. Infrared (IR) spectra were obtained with ABB spectrophotometer, FTLA 2000-100

Compound	ED_{50} (μmol/kg)	
	Leukocyte migration	TNF-α production
ASA	128.0*	N.R.
imatinib	5.0*	0.44*
2c (LASSBio-1597)	5.1*	4.4*
6 (LASSBio-1724)	5.35*	9.26*
7 (LASSBio-1725)	6.1*	8.8*
8 (LASSBio-1726)	3.2*	8.6*
9 (LASSBio-1723)	4.45*	0.07*
10 (LASSBio-1727)	5.4*	0.9*

-N.R. not realized; ASA = acetylsalicylic acid. N=7-10 per group. Doses: 1-50 (μmol/kg). Statistical significance between groups was calculated using analysis of variance (ANOVA) followed by Bonferroni test. P values less than 0.05 (*p < 0.05) were used as significant level.

Table 3: Effects of carboxamides 2c, 6-10, imatinib and acetylsalicylic acid (ASA) in leukocyte migration and TNF-α production induced by carrageenan injection into the subcutaneous air pouch.

model, by using potassium bromide plates. Elemental analysis results were obtained with a Thermo CE scientific apparatus, EA 1112 Series model. Melting points were determined using a Quimis Melting Point Q-340S13 and are uncorrected. Flash chromatography was performed using a LaFlash system (VWR) with Merck silica gel (25-40 μm).

The TLC was performed on 2.0 × 6.0 cm aluminium sheets covered with silica gel (Sorbent, 200 μm thickness) under ultraviolet light (254-365 nm).

The high performance liquid chromatography was performed using Shimadzu – LC20AD with Kromasil column 100-5C18 (4,6 mm × 250 mm), SPD-M20A detector (Diode array) at a wavelength of 254 nm. The mobile phases used: 30% acetonitrile and 70% aqueous trifluoroacetic acid 0,01% or 50% acetonitrile and 50% aqueous trifluoroacetic acid 0,01%

Analyses by differential scanning calorimetry were obtained with DSC-60 Shimadzu. The samples were heated at a rate of 20°C/min, with a temperature range of 30-300°C under a nitrogen flow.

General procedure for the preparation of compounds 4a-c, 11-13 [10]: To a 100 mL flask 6.6 mmol of nitrobenzaldehyde was dissolved in methanol (15 mL). Then, 26.4 mmol of 1-methylpiperazine were added. After 30 minutes, 6.6 moles of sodium cyanoborohydride and 3.3 mol of zinc chloride, previously dissolved in 10 mL of methanol, were added. The mixture was stirred for 2 hours. The end of this step was observed by TLC and desired product was extracted using 20 mL of NaOH 0.1N and 3 × 30 mL of ethyl acetate. Afterwards, organic phases was put together, dried and solvent was evaporated under reduced. The products were purified by column chromatography on silica gel (eluent *n*-hexane:Ethyl Acetate 50:50).

1-(4-nitrobenzyl)-4-methylpiperazine (4a): Yield: orange oil (41%); ^{1}H NMR (200 MHz, $CDCl_3$) δ 2.26 (s, 3H, CH_3), 2.45 (ls, 8H, Ha and Hb), 3.56 (s, 2H, CH_2), 7.47 (d, 2H, *J* = 8.5 Hz, H3' and H5'), 8.12 (d, 2H, *J* = 8.5 Hz, H4' and H6'); ^{13}C NMR (50 MHz, $CDCl_3$) δ 46.1 (Cc), 53.2 (Ca and Ca'), 55.1 (Cb and Cb'), 62.2 (Cd), 123.6 (C-2 and C-2'), 129.6 (C-3 and C-3'), 146.5 (C-4), 147.3 (C-1); IR (KBr) 3050 cm^{-1} (υ C-H aromatics), 2937 and 2793 cm^{-1} (υ CH_2), 1514 cm^{-1} ($\upsilon_a NO_2$), 1342 cm^{-1} ($\upsilon_s NO_2$), 855 cm^{-1} ($\delta_{out\ of\ the\ plane}$ C-H of aromatic ring *para*-substituted).

1-(3-nitrobenzyl)-4-methylpiperazine (4b): Yield: orange oil (45%); ^{1}H NMR (200 MHz, $CDCl_3$) δ 2.30 (s, 3H, CH_3), 2.48 (ls, 8H, Ha and Hb), 3.60 (s, 2H, CH_2), 7.48 (t, 1H, *J*=7.8 Hz, H5'), 7.68 (d, 1H, *J* = 7.5 Hz, H4'), 8.10 (d, 1H, *J* = 8.1 Hz, H6'), 8.21 (s, 1H, H2'); ^{13}C NMR (50 MHz, $CDCl_3$) δ 46.0 (Cc), 53.1 (Ca and Ca'), 55.1 (Cb and Cb'), 62.0 (Cd), 122.2 (C-6), 123.7 (C-2), 129.1 (C-5), 135.0 (C-4), 140.9 (C-3), 148.5 (C-1); IR (KBr) 3045 cm^{-1} (υ C-H aromatic), 1527 cm^{-1} ($\upsilon_a NO_2$), 1318 cm^{-1} ($\upsilon_s NO_2$), 751 and 689 cm^{-1} ($\delta_{out\ of\ the\ plane}$ C-H of aromatic rings *meta*-substituted).

1-(2-nitrobenzyl)-4-methylpiperazine (4c): Yield: yellow solid (44%); MP: 170-171 °C; ^{1}H NMR (200 MHz, $CDCl_3$) δ 2.25 (s, 3H, CH_3), 2.44 (ls, 8H, Ha and Hb), 3.53 (s, 2H, CH_2), 7.41 (t, 1H, *J* = 7.5 Hz, H4'), 7.60 (d, 1H, *J* = 7.6 Hz, H3'), 8.03 (m, 1H, H5'), 8.14 (ls, 1H, H6'); ^{13}C NMR (50 MHz, $CDCl_3$) δ 46.0 (Cc), 53.0 (Ca and Ca'), 55.1 (Cb and Cb'), 62.0 (Cd), 122.3 (C-2), 123.8 (C-6), 129.3 (C-5), 135.1 (C-4), 140.9 (C-3), 148.5 (C-1); IR (KBr) 2938 and 2797 cm^{-1} (υ CH_2), 1528 cm^{-1} ($\upsilon_a NO_2$), 1356 cm^{-1} ($\upsilon_s NO_2$).

1-(2-nitrobenzyl)-4-phenylpiperazine (11): Yield: yellow solid (71%); MP: 108-109 °C; ^{1}H NMR (200 MHz, $CDCl_3$) δ 2.52 (t, 4H, *J* = 4.9 Hz, Ha), 3.08 (t, 4H, *J* = 4.9 Hz, Hb), 3.78 (s, 2H, CH_3), 6.77 (m, 3H, H3", H4" and H5"), 7.16 (m, 2H, H2" and H6"), 7.31 (m, 1H, , H5'), 7.46 (m, 1H, H4'), 7.57 (d, 1H, *J* = 6.9 Hz, H3'), 7.74 (d, 1H, *J* = 7.9 Hz, H6'); ^{13}C NMR (50 MHz, $CDCl_3$) δ 49.2 (Cb and Cb'), 53.2 (Ca and Ca'), 59.0 (Cc), 116.2 (C-2' and C-6'), 119.8 (C-2), 124. 5 (C-4'), 128.1 (C-6), 129.1 (C-3' and C-5'), 131.1 (C-5), 132.5 (C-4), 133.5 (C-3), 150.0 (C-1), 151.3 (C-1'); IR (KBr) 2952 and 2817 cm^{-1} (υ CH_2), 1596, 1492 and 1443 cm^{-1} (υ C=C aromatic), 1525 cm^{-1} ($\upsilon_a NO_2$), 1348 cm^{-1} ($\upsilon_s NO_2$).

1-(2-nitrobenzyl)-4-(2-pyrimidyl)piperazine (12): Yield: white solid (71%); MP: 110-112 °C; ^{1}H NMR (200 MHz, $CDCl_3$) δ 2.37 (t, 4H, *J* = 4.6 Hz, Ha), 3.65 (t, 4H, *J* = 4.5 Hz, Hb), 3.75 (s, 2H, CH_2), 6.60 (t, 1H, *J* = 4.6 Hz, H4"), 7.48 – 7.56 (m, 1H, H3' and H5'), 7.65 (m, 2H, H4'), 7.87 (d, 1H, *J* = 7.8 Hz, H6'), 8.32 (m, 2H, H3" and H5"); ^{13}C NMR (50 MHz, $CDCl_3$) δ 43.8 (Cb and Cb'), 53.0 (Ca and Ca'), 58.7 (Cc), 110.7 – 161.6 (C-aromatics); IV (KBr) 2936 and 2821 cm^{-1} (υ CH_2), 1587, 1498 and 1446 cm^{-1} (υ C=C aromatic), 1541 cm^{-1} ($\upsilon_a NO_2$), 1355 cm^{-1} ($\upsilon_s NO_2$).

1-(2-nitrobenzyl)-4-(2-hydroxyethyl)piperazine (13): Yield: yellow oil (47%); ^{1}H NMR (200 MHz, $CDCl_3$) δ 2.43 – 2.50 (m, 8H, Ha and Hb), 2.74 (ls, 2H, Hd), 3.54 (t, 2H, *J* = 5.3 Hz, He), 3.73 (s, 2H, CH_2), 7.28 – 7.36 (m, 1H, H4'), 7.42 – 7.52 (m, 2H, H3' and H5'), 7.73 (d, 1H, *J* = 7.7 Hz, H6'); ^{13}C NMR (50 MHz, $CDCl_3$) δ 53.0 (Ca and Ca'), 53.1 (Cb and Cb'), 57.8 (Cc), 59.1 (Cd), 59.4 (Ce), 124.5 (C-2), 128.1 (C-6), 131.1 (C-5), 132.4 (C-4), 133.8 (C-3), 150.0 (C-1); IV (KBr) 3390 cm^{-1} (υ_a OH), 2940 and 2816 cm^{-1} (υ CH_2), 1529 cm^{-1} ($\upsilon_a NO_2$), 1356 cm^{-1} ($\upsilon_s NO_2$).

General procedure for preparation of intermediates 5a-c, 14-16 [11]: To a 125 mL flask containing 1.3 mmol of nitro-compound and 90 mL of ethanol:water (2:1) were added 7.3 mmol of iron powder and 2.1 mmol of ammonium chloride. The mixture was refluxed for 1 hour. The hot mixture was filtered through Celite and concentrated *in vacuo*. The residue was diluted with H_2O and extracted with AcOEt. Afterwards, organic phases was dried over anhydrous Na_2SO_4 and concentrated to give the amine intermediates.

4-[(4-methylpiperazin-1-yl)methyl]benzenamine (5a): Yield: yellow solid (83%); MP: 68-70 °C; ^{1}H NMR (200 MHz, $CDCl_3$) δ 2.27 (s, 3H, CH_3), 2.44 (ls, 8H, Ha and Hb), 3.39 (s, 2H, CH_2), 3.51 (s, 2H, NH_2), 6.62 (d, 2H, *J* = 7.9 Hz, H3' and H4'), 7.08 (d, 2H, *J* = 7.8 Hz, H2' and H6'); ^{13}C NMR (50 MHz, $CDCl_3$) δ 46.1 (Cc), 53.0 (Ca and Ca'), 55.2 (Cb and Cb'), 62.7 (Cd), 114.9 (C-2 and C-2'), 129.0 (C-4), 130.4 (C-3 and C-3'), 145.5 (C-1); IV (KBr) 3444 cm^{-1} ($\upsilon_a NH_2$), 3361 cm^{-1} ($\upsilon_s NH_2$), 2933 and 2807 cm^{-1} (υ CH_2), 1621, 1518 and 1450 cm^{-1} (υ C=C aromatic), 826 cm^{-1} ($\delta_{out\ of\ the\ plane}$ C-H of aromatic rings *para*-substituted).

3-[(4-methylpiperazin-1-yl)methyl]benzenamine (5b): Yield: yellow solid (78%); MP: 70-71 °C; ^{1}H NMR (200 MHz, $CDCl_3$) δ 2.20 (s, 3H, CH_3), 2.38 (ls, 8H, Ha and Hb), 3.33 (s, 2H, CH_2), 3.53 (m, 2H, NH_2), 6.47 (m, 1H, H2'), 6.61 (d, 2H, *J* = 7.0 Hz, H4' and H6'), 7.00 (t, 1H, *J* = 7.7 Hz, H5'); ^{13}C NMR (50 MHz, $CDCl_3$) 46.1 (Cc), 53.2 (Ca and Ca'), 55.2 (Cb and Cb'), 63.1 (Cd), 113.9 (C-6), 115.8 (C-2), 119.5 (C-4), 129.1 (C-5), 139.5 (C-3), 146.5 (C-1); IV (KBr) 3408 cm^{-1} ($\upsilon_a NH_2$), 3307 cm^{-1} ($\upsilon_s NH_2$), 2946 and 2794 cm^{-1} (υ CH_2), 1606, 1494 and 1454 cm^{-1} (υ C=C aromatic), 783 and 692 cm^{-1} ($\delta_{out\ of\ the\ plane}$ C-H of aromatic rings *meta*-substituted).

2-[(4-methylpiperazin-1-yl)methyl]benzenamine (5c): Yield: yellow solid (74%); MP: 85-87 °C; ^{1}H NMR (200 MHz, $CDCl_3$) δ 2.21 (s, 3H, CH_3), 2.37 (ls, 8H, Ha and Hb), 3.44 (s, 2H, CH_2), 4.51 (s, 2H, NH_2), 6.58 (m, 2H, *J* = 8.0 Hz, H4' and H5'), 6.89 – 7.05 (m, 2H, H3' and H6'); ^{13}C NMR (50 MHz, $CDCl_3$) δ 46.1 (Cc), 52.7 (Ca and Ca'), 55.4 (Cb and Cb'), 62.0 (Cd), 115.6 (C-6), 117.7 (C-4), 122.4 (C-2), 128.5 (C-3), 130.6 (C-5), 147.1 (C-1); IV (KBr) 3364 cm^{-1} ($\upsilon_a NH_2$), 3303 cm^{-1}

(υ_s NH_2), 2938 and 2806 cm^{-1} (υ CH_2), 750 cm^{-1} ($\delta_{out\ of\ the\ plane}$ C-H of aromatic rings *ortho*-substituted).

2-[(4-phenylpiperazin-1-yl)methyl]benzenamine (14): Yield: white solid (84%); MP: 178-179 °C; ^{1}H NMR (200 MHz, $CDCl_3$) δ 2.51 (t, 4H, *J* = 4.9 Hz, Ha), 3.09 (t, 4H, *J* = 4.9 Hz, Hb), 3.50 (s, 2H, CH_2), 4.51 (ls, NH_2), 6.54 – 7.21 (9H, H-aromatics); ^{13}C NMR (50 MHz, $CDCl_3$) δ 49.4 (Cb and Cb'), 52.9 (Ca and Ca'), 62.0 (Cc), 115.8 (C-6), 116.2 (C-2' and C-6'), 117.8 (C-4), 119.9 (C-4'), 121.9 (C-2), 128.8 (C-3), 129.3 (C-3' and C-5'), 130.8 (C-5), 147.2 (C-1), 151.4 (C-1'); IV (KBr) 3443 cm^{-1} (υ_a NH_2), 3311 cm^{-1} (υ_s NH_2), 2932 and 2817 cm^{-1} (υ CH_2), 1599, 1498 and 1451 cm^{-1} (υ C=C aromatic), 746 cm^{-1} ($\delta_{out\ of\ the\ plane}$ C-H of aromatic rings *ortho*-substituted).

2-{[4-(pyrimidin-2-yl)piperazin-1-il]methyl}benzenamine (15): Yield: yellow solid (81%); MP: 100-102 °C; ^{1}H NMR (200 MHz, $CDCl_3$) δ 2.44 (t, 4H, *J* = 5.0 Hz, Ha), 3.50 (s, 2H, CH_2), 3.75 (t, 4H, *J* = 4.9 Hz, Hb), 6.41 (t, 1H, *J* = 4.7 Hz, H4"), 6.61 (t, 2H, *J* = 6.9 Hz, H3' and H5'), 6.92 (d, 1H, *J* = 6.6 Hz, H6'), 7.05 (t, 1H, *J* = 8.2 Hz, H4'), 8.22 (d, 2H, *J* = 4.7 Hz, H3" and H5"); ^{13}C NMR (50 MHz, $CDCl_3$) δ 43.9 (Cb and Cb'), 52.8 (Ca and Ca'), 62.1 (Cc), 110.1 (C-5'), 115.9 (C-6), 117.9 (C-4), 121.7 (C-2), 128.9 (C-3), 130.9 (C-5), 147.2 (C-1), 157.9 (C-4' and C-6'), 161.8 (C-2'); IV (KBr) 3421 cm^{-1} (υ_a NH_2), 3302 cm^{-1} (υ_s NH_2), 2929 and 2814 cm^{-1} (υ CH_2), 1586, 1495 and 1448 cm^{-1} (υ C=C aromatic), 751 cm^{-1} ($\delta_{out\ of\ the\ plane}$ C-H of aromatic rings *ortho*-substituted).

2-[(4-hydroxyethyl-piperazin-1-yl)methyl]benzenamine (16): Yield: yellow solid (76%); MP: 63-65 °C; ^{1}H NMR (200 MHz, $CDCl_3$) δ 2.43 – 2.50 (m, 10H, Ha, Hb and Hd), 3.44 (s, 2H, CH_2), 3.55 (t, 2H, *J* = 5.6 Hz, He), 4.03 (ls, 2H, NH_2), 6.58 (t, 2H, *J* = 8.2 Hz, H4' and H5'), 6.93 (d, 1H, *J* = 7.1 Hz, H3'), 7.01 (t, 1H, *J* = 7.6 Hz, H6'); ^{13}C NMR (50 MHz, $CDCl_3$) δ 52.7 (Ca and Ca'), 53.2 (Cb and Cb'), 57.9 (Cc), 59.5 (Cd), 62.0 (Ce), 115.6 (C-6), 117.7 (C-4), 122.2 (C-2), 128.5 (C-3), 130.6 (C-5), 147.0 (C-1); IV (KBr) 3373 cm^{-1} (υ_a OH), 3307 cm^{-1} (υ_a NH_2), 3212 cm^{-1} (υ_s NH_2), 2942 and 2817 cm^{-1} (υ CH_2), 1634, 1495 and 1456 cm^{-1} (υ C=C aromatic), 762 cm^{-1} ($\delta_{out\ of\ the\ plane}$ C-H of aromatic rings *ortho*-substituted).

General procedure for preparation of the compounds 2a-c, 6-10 [12]: To a flask of the 50 mL containing 1 mmol of acyl chloride derivative in dichloromethane (20mL) treated with 2.2 mmol of triethylamine was added 1 mmol of amine-compound and the mixture stirred at room temperature for 2 hours. The mixture was diluted with additional dichloromethane (10 mL) and brine (20 mL) and washed with 0.05M HCl (10 mL) and brine (20 mL). The organic portion was dried (Na_2SO_4), filtered and concentrate *in vacuo*.

N-{4-[(4-methylpiperazin-1-yl)methyl]phenyl}quinoxaline-2-carboxamide (2a; LASSBio-1599): Yield: yellow solid (64%). When necessary, the product was purified by flash chromatography on silica gel (elution with 1% triethylamine in ethyl acetate); MP: 156 °C; ^{1}H NMR (200 MHz, $CDCl_3$) δ 2.26 (s, 3H, CH_3), 2.47 (ls, 8H, Ha and Hb), 3.44 (s, 2H,CH_2), 7.19 (d, 2H, *J* = 8.2 Hz, H3' and H5'), 9.70 (d, 2H, *J* = 8.2 Hz, H2' and H6'), 7.77 – 7.82 (m, 2H, H5 and H8), 8.07 – 8.15 (m, 2H, H6 and H7), 9.67 (s, 1H, H3), 9.75 (s, 1H, CONH); ^{13}C NMR (50 MHz, $CDCl_3$) δ 46.0 (Cc), 53.0 (Cb and Cb'.), 55.2 (Ca and Ca'), δ62.6 (Cd), 119. 9 (C-2 and C-6), 129.7 (C-6'), 130.1 (C-3 and C-5), 131.2 (C-8'), 132.0 (C-9'), 134.9 (C-7'), 136.4 (C-4), 140.2 (C-1), 143.5 (C-10'), 144.0 (C-2'), 144.2 (C-3' and C-5'), 161.0 (CONH); IR (KBr) 3280 cm^{-1} (υ CONH), 2931 and 2793 cm^{-1} (υ CH_2), 1682 cm^{-1} (υ CONH), 830 cm^{-1} ($\delta_{out\ of\ the\ plane}$ C-H of aromatic rings *para*-substituted); Elementar Analysis $C_{21}H_{23}N_5O$ (361): Calculated - C, 69.44; H, 6.41; N, 19.38. Found – C, 69.78; H, 6.60; N, 18.98.

N-{3-[(4-methylpiperazin-1-yl)methyl]phenyl}quinoxaline-2-carboxamide (2b; LASSBio-1598): Yield: yellow solid (53%). When necessary, the product was purified by flash chromatography on silica gel (elution with 1% triethylamine in ethyl acetate); MP: 142 °C; ^{1}H NMR (200 MHz, $CDCl_3$) δ 2.27 (s, 3H, CH_3), 2.49 (ls, 8H, Ha and Hb), 3.49 (s, 2H, CH_2), 7.07 (d, 1H, *J* = 7.4 Hz, H4'), 7.30 (t, 1H, *J* = 7.7 Hz, H5'), 7.65 (s, 1H, H6'), 7.74 (s, 1H, H2'), 7.79 – 7.84 (m, 2H, H6 and H7), 8.09 – 8.16 (m, 2H, H5 and H8), 9.69 (s, 1H, H3), 9.79 (s, 1H, CONH); ^{13}C NMR (50 MHz, $CDCl_3$) δ 45.8 (Cc), 52.8 (Cb and Cb'.), 55.0 (Ca and Ca'), 62.8 (Cd), 118.8 – 144.1 (14C, C-aromatic), 161.0 (CONH); IV (KBr) 3257 cm^{-1} (υ CONH), 2945 and 2794 cm^{-1} (υ CH_2), 1680 cm^{-1} (υ CONH) 1607, 1537 and 1488 cm^{-1} (υ C=C aromatic); Elementar Analysis $C_{21}H_{23}N_5O$ (361): Calculated - C, 69.44; H, 6.41; N, 19.38. Found – C, 69.32; H, 6.18; N, 19.38.

N-{2-[(4-methylpiperazin-1-yl)methyl]phenyl}quinoxaline-2-carboxamide (2c; LASSBio-1597): Yield: yellow solid (51%). When necessary, the product was purified by flash chromatography on silica gel (elution with 1% triethylamine in ethyl acetate); MP: 132 °C; ^{1}H NMR (200 MHz, $CDCl_3$) δ 2.30 (s, 3H, CH_3), 2.64 (ls, 8H, Ha and Hb), 3.64 (s, 2H, CH_2), 6.99 – 8.43 (m, 8H, H-aromatics), 9.69 (s, 1H, H3'), 11.70 (s, 1H, CONH); ^{13}C NMR (50 MHz, $CDCl_3$) δ 45.7 (Cc), 52.3 (Cb and Cb'.), 55.1 (Ca and Ca'), 61.5 (Cd), 121.9 – 145.03 (14C, C-aromatics), 162.0 (CONH); IR (KBr) 3238 cm^{-1} (υ CONH), 2933 and 2795 cm^{-1} (υ CH_2), 1684 cm^{-1} (υ CONH) 1590, 1525 and 1450 cm^{-1} (υ C=C aromatic), 753 cm^{-1} ($\delta_{out\ of\ the\ plane}$ C-H of aromatic rings *ortho*-substituted); Elementar Analysis $C_{21}H_{23}N_5O$ (361): Calculated - C, 69.78; H, 6.41; N, 19.38. Found: C, 69.44; H, 5.99; N, 19.21; HPLC (C-18, acetonitrile: aqueous trifluoroacetic acid (30:70), 254 nm): Retention time: 7.64 min. Peak Area: 98.928 %.

N-{2-[(4-methylpiperazin-1-yl)methyl]phenyl}pyrazine-2-carboxamide (6; LASSBio-1724): Yield: yellow solid (72%). When necessary, the product was purified by flash chromatography on silica gel (elution with 1% triethylamine in ethyl acetate); MP: 134 °C; ^{1}H NMR (200 MHz, $CDCl_3$) δ 2.35 (s, 3H, CH_3), 2.62 (ls, 8H, Ha and Hb), 3.59 (s, 2H, CH_2), 6.98 – 7.13 (m, 2H, H3' and H4'), 7.30 (t, 1H, *J* = 7.0 Hz, H5), 8.37 (d, 1H, *J* = 8.0 Hz, H6'), 8.52 (s, 1H, H6), 8.72 (d, 1H, *J* = 2.3 Hz, H5), 9.45 (s, 1H, H3), 12.12 (s, 1H, CONH); ^{13}C NMR (50 MHz, $CDCl_3$) δ 45.7 (Cc), 52.1 (Cb and Cb'.), 54.8 (Ca and Ca'), 61.6 (Cd), 121.5 (C-6), 124.2 (C-4), 126.8 (C-5), 128.7 (C-3), 130.2 (C-2), 137.9 (C-1), 142.5 (C-3'), 145.2 (C-5'), 145.8 (C-2'), 147.2 (C-6'), 161.5 (CONH); IR (KBr) 3456 cm^{-1} (υ CONH), 2937 and 2795 cm^{-1} (υ CH_2), 1677 cm^{-1} (υ CONH) 1590, 1534 and 1452 cm^{-1} (υ C=C aromatic), 756 cm^{-1} ($\delta_{out\ of\ the\ plane}$ C-H of aromatic rings *ortho*-substituted); HPLC (C-18, acetonitrile: aqueous trifluoroacetic acid (30:70), 254 nm): Retention time: 3.136 min. Peak Area: 95.355 %.

N-{2-[(4-methylpiperazin-1-yl)methyl]phenyl}quinoxaline-6-carboxamide (7; LASSBio-1725): Yield: yellow solid (64%). When necessary, the product was purified by flash chromatography on silica gel (elution with 1% triethylamine in ethyl acetate); MP: 128 °C; ^{1}H NMR (200 MHz, $CDCl_3$) δ 2.31 (s, 3H, CH_3), 2.59 (sl, 8H, Ha and Hb), 3.66 (s, 2H, CH_2), 6.97 – 7.13 (m, 2H, H3' and H4'), 7.31 (t, 1H, *J* = 8.3 Hz, H5'), 8.16 (d, 1H, *J* = 8.7 Hz, H6'), 8.31 – 8.42 (m, 2H, H4 and H5), 8.62 (s, 1H, H7), 8.86 (s, 2H, H9 and H10), 11.61 (s, 1H, CONH); ^{13}C NMR (50 MHz, $CDCl_3$) δ 45.6 (Cc), 52.5 (Cb e Cb'), 54.7 (Ca e Ca'), 62.4 (Cd), 121.0 – 146.4 (14C, C-aromáticos), 164.2 (CONH); IR (KBr) 3467 cm^{-1} (υ CONH), 2937 e 2809 cm^{-1} (υ CH_2), 1672 cm^{-1} (υ CONH) 1591, 1529 e 1448 cm^{-1} (υ C=C aromático), 749 cm^{-1} ($\delta_{out\ of\ the\ plane}$ C-H aromatic rings *ortho*-substituted); HPLC (C-18, acetonitrile: aqueous trifluoroacetic acid (30:70), 254 nm): Retention time: 3.688 min. Peak Area: 95.913 %.

N-{2-[(4-phenylpiperazin-1-yl)methyl]phenyl}quinoxaline-2-carboxamide (8; LASSBio-1726): Yield: yellow solid (59%). When necessary, the product was purified by flash chromatography on silica gel (elution with 20% ethyl acetate in *n*-hexane); MP: 179 ºC; ^{1}H NMR (200 MHz, $CDCl_3$) δ 2.69 (t, 4H, *J* = 4.5 Hz, Ha), 3.29 (t, 4H, *J* = 4.7 Hz, Hb), 3.67 (s, 2H, CH_2), 6.74 – 8.42 (13H, H-aromatics), 9.66 (s, 1H, H3), 11.90 (s, 1H, CONH); ^{13}C NMR (50 MHz, $CDCl_3$) δ49.4 (Cb and Cb'), 53.0 (Ca and Ca'), 62.0 (Cc), 116.3 – 151.3 (20C, C-aromatics), 162.3 (CONH); IR (KBr) 3217 cm^{-1} (υ CONH), 2938 and 2825 cm^{-1} (υ CH_2), 1679 cm^{-1} (υ CONH) 1591, 1527 and 1452 cm^{-1} (υ C=C aromatic), 754 cm^{-1} ($\delta_{out\ of\ the\ plane}$ C-H of aromatic rings *ortho*-substituted); HPLC (C-18, acetonitrile: aqueous trifluoroacetic acid (50:50), 254 nm): Retention time: 5.055 min. Peak Area: 97.413 %.

N-{2-[(4-(pyrimidin-2-yl)piperazin-1-yl)methyl]phenyl} quinoxaline-2-carboxamide (9; LASSBio-1723): Yield: yellow solid (58%). When necessary, the product was purified by flash chromatography on silica gel (elution with 30% ethyl acetate in *n*-hexane); MP: 216 ºC; ^{1}H NMR (200 MHz, $CDCl_3$) δ 2.60 (ls, 4H, Ha), 3.66 (s, 2H, CH_2), 3.92 (ls, 4H, Hb), 6.39 – 8.47 (11H, H-aromatics), 9.72 (s, 1H, H3), 11.91 (s, 1H, CONH); ^{3}C NMR (50 MHz, $CDCl_3$) δ 44.0 (Cb and Cb'), 52.8 (Ca and Ca'), 62.0 (Cc), 110.1 – 161.7 (18C, C-aromatics), 162.2 (CONH); IV (KBr) 3221 cm^{-1} (υ CONH), 2930 and 2817 cm^{-1} (υ CH_2), 1681 cm^{-1} (υ CONH) 1585, 1539 and 1447 cm^{-1} (υ C=C aromatic), 753 cm^{-1} ($\delta_{out\ of\ the\ plane}$ C-H of aromatic rings *ortho*-substituted); HPLC (C-18, acetonitrile: aqueous trifluoroacetic acid (50:50), 254 nm): Retention time: 3.300 min. Peak Area: 98.053 %.

N-{2-[(4-(2-hydroxyethyl)piperazin-1-yl)methyl]phenyl} quinoxaline-2-carboxamide (10; LASSBio-1727): Yield: yellow solid (62%). When necessary, the product was purified by flash chromatography on silica gel (elution with ethyl acetate); MP: 150 ºC; ^{1}H NMR (200 MHz, $CDCl_3$) δ 2.65 (ls, 8H, Ha and Hb), 3.11 (ls, 2H, Hc), 3.59 (t, 3H, *J* = 5.0 Hz, He and Hf), 3.64 (s, 2H, CH_2), 7.00 – 8.44 (8H, H-aromatics), 9.70 (s, 1H, H3), 11.75 (s, 1H, CONH); ^{13}C NMR (50 MHz, $CDCl_3$) δ 52.7 (Ca and Ca'), 53.1 (Cb and Cb'), 57.8 (Cd), 59.4 (Cc), 61.6 (Ce), 121.9 – 145.0 (14C, C-aromatics), 162.0 (CONH); IR (KBr) 3390 cm^{-1} (υ_a OH), 3213 cm^{-1} (υ CONH), 2934 and 2812 cm^{-1} (υ CH_2), 1680 cm^{-1} (υ CONH) 1591, 1538 and 1452 cm^{-1} (υ C=C aromatic), 755 cm^{-1} ($\delta_{out\ of\ the\ plane}$ C-H of aromatic rings *ortho*-substituted); HPLC (C-18, acetonitrile: aqueous trifluoroacetic acid (50:50), 254 nm): Retention time: 6.463 min. Peak Area: 98.748 %.

X-ray crystallography

Single crystals of the compounds 2a-c (Table 4), suitable for X-ray study, were obtained by slow evaporation of a solution of ethanol-dimethylformamide (3:1), ethanol-dimethyl sulfoxide-dichloromethane (1:1:1) and methanol:dichloromethane (10:1), respectively, at room temperature 295(2) K. Data collection was performed using the Kappa Apex II Duo diffractometer operating with Mo-Kα radiation (λ=0.71073 Å) an room temperature. Raw data integration was performed with Saint (Bruker, 2009) and the scaling were carried out using SADABS (Bruker, 2009). Structure solution was obtained using Direct Methods implemented in SHELXS and the model refinement was performed with full matrix least squares on F^2 using SHELXL. The programs ORTEP-3, [13] SHELXS/SHELXL [18] were used within WinGX [19] software package.

Compound	2a	2b	2c
Crystal system	Monoclinic	Monoclinic	Monoclinic
Space group	$P2_1/c$	$P2_1/c$	$P2_1/c$
Unit cell dimensions			
a(Å)	17.651(4)	6.3082(3)	5.7947(12)
b(Å)	5.8253(14)	26.4257(14)	16.576(4)
c(Å)	19.925(4)	11.5607(6)	20.465(4)
β(°)	108.344(7)	98.802(3)	106.312(11)
Volume (Å^3)	1944.6(7)	1904.46(17)	1886.7(7)
Z	4	4	4
Density Calculated (Mg/m^3)	1.235	1.261	1.272
Absorption coefficient (mm^{-1})	0.079	0.081	0.082
F(000)	768	768	768
Crystal size (mm^3)	0.25x0.2x0.2	0.32x0.19x0.04	0.41x0.14x0.07
θ range (°)	2.11 to 26.23	1.54 to 25.39	1.61 to 26.47
Index ranges			
h	-21 to 21	-7 to 7	-7 to 7
k	-7 to 7	-30 to 31	-19 to 20
l	-24 to 15	-13 to 13	-25 to 23
Reflections collected	14313	9930	14347
Independent reflections	3881	3410	3858
R(int)	0.0459	0.0500	0.0223
Completeness to θ = 25° (%)	99.1	99.3	99.2
Data / restraints / parameters	3881 / 0 / 245	3410 / 0 / 244	3858 / 0 / 246
Goodness-of-fit on F^2	1.064	1.021	1.044
Final R1 indices [I>2σ(I)]	0.0410	0.0542	0.0399
Final wR2 indices [I>2σ(I)]	0.1276	0.1325	0.1059
R indices (all data)	0.0577	0.0908	0.0544
R indices (all data)	0.1442	0.1532	0.1146
Extinction coefficient	0.0113(19)		0.0083(12)
Largest diff. peak / hole (e.Å^{-3})	0.214 / -0.174	0.156 / -0.167	0.168 / -0.152

Table 4: Crystal data and structure refinement details of compounds 2a-c.

Biological assays

All experiments were performed with male Swiss mice (20-25 g) obtained from Instituto Vital Brazil (Niterói, Brazil). Animals were maintained in temperature-controlled room (22 ± 2°C) with a 12 h light/dark cycles and free access to food and water. Twelve hours prior to each experiment, the animals received only water in order to avoid food interfering with the substance absorption. Animal care and research protocols (DFBCICB015-04/16) were in accordance with the principles and guidelines adopted by the National Council of Control of Animal Experimentation (CONCEA).

MTT assay [14]: The tumor cells used HL-60 (human leukemia – ATCC code: CCL-240™), HCT-8 (human colorectal carcinoma – ATCC code: CCL-244™) and SF-295 (human glioblastoma) were provided by the National Cancer Institute (USA). Human lymphocytes were isolated from heparinized blood from healthy, non-smoker donors who had not taken any medication at least 15 days prior to sampling by a standard method of density-gradient centrifugation on Histopaque-1077 (Sigma Aldrich Co. - St. Louis, MO/USA). Cancer cells and lymphocytes were incubated in RPMI 1640 supplemented with 10% (tumor cells) or 20% (lymphocytes) fetal calf serum. Lymphocytes cultures were also supplemented with 2% phytohaemagglutinin. Cells were seeded in 96 well plates at the following densities: 0.3×10^6 (HL-60), 0.7×10^5 (HCT8, SF-295), and 1×10^6 (lymphocytes) cells/mL. After 24 hour, the compounds were added at concentrations ranging from 0.1 μM – 300 μM and then incubated at 37°C and atmosphere containing 5% CO_2 for 72 hours. After that, it was added 100 μL of a solution of MTT (5 mg/mL) in RPMI medium and incubated for 3 hour at the same conditions. After incubation time, it was added 100 μL of DMSO for solubilization of MTT-formazan crystals formed by the metabolism of MTT salt by the viable cells. Finally, the plates were read on an ELISA reader at a wavelength of 550 nm.

The experiments were analyzed according to their means and standard error media (S.E.M.) confidence intervals from nonlinear regression in GraphPad Prism. Each sample was tested in triplicate in two independent experiments.

Air pouch synovial model [15]: The method was similar to that described by Romano et al. [16] with several modifications described in Raymundo et al. [17]. Briefly, air pouches were produced by subcutaneous injection of sterile air (10 ml) into the intrascapular region of the mice. After three days, another injection of air (10 ml) was performed in order to maintain the pouches. Three days after the last injection of air, animals received an injection of sterile carrageenan suspension (1%) into the SAP. Mice were pre-treated with oral doses of substances, ASA or vehicle 1 h before carrageenan injection in the SAP. Animals were sacrificed 24 h after carrageenan injection and the cavity was washed with 1 ml of sterile PBS. The total number of cells was determined with the aid of a haemocytometer (CellPoucH, Merck, USA). The exudates were centrifuged at 170 x g for 10 min at 4 °C, and the supernatants were collected and stored at –20°C to further analysis. Supernatants from exudates collected in the SAP were used to measure tumor necrosis factor-α (TNF-α) by enzyme-linked immunosorbent assay (ELISA), using the protocol supplied by the manufacturer (B&D, USA).

Statistical analysis

The results are presented as mean ± standard deviation (SD), mean ± error deviation or mean ± confidence interval using the GraphPad Prism vs. 5.0. Statistical significance between groups was calculated using analysis of variance (ANOVA) followed by Bonferroni or Dunnet tests. P values less than 0.05 (*$p<0.05$) were used as significant level.

Acknowledgments

The authors would like to thank INCT-INOFAR (573.564/2008-6 and E-26/170.020/2008), CNPq (BR), FAPERJ (BR) and CAPES (BR) for fellowship and financial support. We also thank Dr. Nailton Monteiro do Nascimento Júnior for his valuable help with the NMR spectra analysis.

References

1. Capdeville R, Buchdunger E, Zimmermann J, Matter A (2002) Glivec (STI57, imatinib), a rationally developed, targeted anticancer drug. Nat Rev Drug Discov 1: 493-502.
2. Lydon NB, Druker BJ (2004) Leukemia Res 28S: 29-38.
3. Akhmetshina A, Venalis P, Dees C, Busch N, Zwerina J, et al. (2009) Treatment with imatinib prevents fibrosis in different preclinical models of systemic sclerosis and induces regression of established fibrosis. Arthritis & Rheumatism 60: 219-224.
4. Kim I, Rhee C, Yeo C, Kang H, Lee D, et al. (2013) 17: R114.
5. Huang P, Zhao XS, Fields M, Ransohoff RM, Zhou L (2009) Imatinib attenuates skeletal muscle dystrophy in mdx mice. FASEB J 23: 2539-2548.
6. Wolf AM, Wolf D, Rumpold H, Ludwiczek S, Enrich B, et al. (2005) The kinase inhibitor imatinib mesylate inhibits TNF-{alpha} production in vitro and prevents TNF-dependent acute hepatic inflammation. Proc Natl Acad Sci U S A 102: 13622-13627.
7. Miyachi K, Ihara A, Hankins RW, Murai R, Maehiro S, et al. (2003) Efficacy of imatinib mesylate (STI571) treatment for a patient with rheumatoid arthritis developing chronic myelogenous leukemia. Clin Rheumatol 22: 329-332.
8. Barreiro EJ (2002) Estratégia De Simplificação Molecular No Planejamento Racional De Fármacos: A Descoberta De Novo Agente Cardioativ. Quimica Nova 25: 1172-1180.
9. Lima LM, Barreiro EJ (2005) Bioisosterism: a useful strategy for molecular modification and drug design. Curr Med Chem 12: 23-49.
10. Kim S, Oh CH, Ko JS, Ahn KH, Kim YJ (1985) Zinc-modified cyanoborohydride as a selective reducing agent. J Org Chem 50: 1927-1932.
11. Li CS, Black WC, Chan CC, Ford-Hutchinson AW, Gauthier JY, et al. (1995) Cyclooxygenase-2 Inhibitors. Synthesis and Pharmacological Activities of 5-Methanesulfonamido-1-indanone Derivatives. J Med Chem 38: 4897-4905.
12. Kort ME, Drizin I, Gregg RJ, Scanio MJC, Shi L, et al. (2008) Discovery and Biological Evaluation of 5-Aryl-2-furfuramides, Potent and Selective Blockers of the $Na_v1.8$ Sodium Channel with Efficacy in Models of Neuropathic and Inflammatory Pain. J Med Chem 5: 407-416.
13. Farrugia LJ (1997) ORTEP-3 for Windows - a version of ORTEP-III with a Graphical User Interface (GUI). J Appl Cryst 30: 565.
14. Mosmann T (1983) Rapid colorimetric assay for cellular growth and survival: application to proliferation and cytotoxicity assays. J Immunol Methods 65: 55-63.
15. Edwards JC, Sedgwick AD, Willoughby DA (1981) The formation of a structure with the features of synovial lining by subcutaneous injection of air: an in vivo tissue culture system. J Pathol 134: 147-156.
16. Romano M, Faggioni R, Sironi M, Sacco S, Echtenacher B, et al. (1997) Carrageenan-induced acute inflammation in the mouse air pouch synovial model. Role of tumour necrosis factor. Mediators Inflamm 6: 32-38.
17. Raymundo LJ, Guilhon CC, Alviano DS, Matheus ME, Antoniolli AR, et al. (2011) Characterisation of the anti-inflammatory and antinociceptive activities of the Hyptis pectinata (L.) Poit essential oil. J Ethnopharmacol 134: 725-732.
18. Sheldrick GM (2008) A short history of SHELX. Acta Crystallogr A 64: 112-122.
19. Farrugia LJ (1999) WinGX suite for small-molecule single-crystal crystallography. J Appl Crystallogr 32: 837-828.